

Journal of Materials Chemistry A

Accepted Manuscript



This is an *Accepted Manuscript*, which has been through the Royal Society of Chemistry peer review process and has been accepted for publication.

Accepted Manuscripts are published online shortly after acceptance, before technical editing, formatting and proof reading. Using this free service, authors can make their results available to the community, in citable form, before we publish the edited article. We will replace this *Accepted Manuscript* with the edited and formatted *Advance Article* as soon as it is available.

You can find more information about *Accepted Manuscripts* in the [Information for Authors](#).

Please note that technical editing may introduce minor changes to the text and/or graphics, which may alter content. The journal's standard [Terms & Conditions](#) and the [Ethical guidelines](#) still apply. In no event shall the Royal Society of Chemistry be held responsible for any errors or omissions in this *Accepted Manuscript* or any consequences arising from the use of any information it contains.



Direct Electron Transfer-Type Dual Gas Diffusion H₂/O₂ Biofuel Cells

Received 00th January 20xx,
Accepted 00th January 20xx

Keisei So,^a Yuki Kitazumi,^a Osamu Shirai,^a Koji Nishikawa,^b Yoshiki Higuchi,^b and Kenji Kano*^a

DOI: 10.1039/x0xx00000x

Received _____

www.rsc.org/

H₂/O₂ biofuel cells utilizing hydrogenases and multicopper oxidases as bioelectrocatalysts are clean, sustainable, and environmentally friendly power devices. In this study, we constructed a novel gas diffusion bioelectrode with a sheet of waterproof carbon cloth as the electrode base and optimized the hydrophilicity/hydrophobicity of the electrode for both high gas permeability and high direct electron transfer bioelectrocatalytic activity. The electrode exhibited a large current density of about 10 mA cm⁻² in the steady state for both H₂ oxidation and O₂ reduction. The biocathode and the bioanode were coupled to construct a gas diffusion H₂/O₂ biofuel cell. The dual gas diffusion system allowed the separate supply of gaseous substrates (H₂ and O₂) to the bioanode and biocathode, with consequent suppression of the oxidative inhibition of the hydrogenases. The cell exhibited a maximum power density of 8.4 mW cm⁻² at a cell voltage of 0.7 V under quiescent conditions.

Introduction

Biofuel cells are energy conversion systems in which enzymes are utilized as biocatalysts.¹⁻⁸ Due to the characteristics of the enzyme reaction, the power device can operate under very mild and safe conditions, e.g., at neutral pH, room temperature, and atmospheric pressure.¹⁻⁸ Moreover, the active sites in enzymes consist of nonprecious metals (e.g., Cu, Ni, Fe, Mo, and W) or organic compounds (e.g., nicotinamide adenine dinucleotide, flavin adenine dinucleotide, and quinones).⁷⁻¹¹ Although conventional polymer electrolyte H₂/O₂ fuel cells are known as clean and efficient energy conversion devices, they usually require Pt catalysts, which are expensive.¹²⁻¹⁴ By utilizing hydrogenases^{11,15,16} and multicopper oxidases (MCOs)¹⁰ as catalysts for H₂ oxidation and O₂ reduction, respectively, a sustainable and environmentally friendly H₂/O₂ biofuel cell may be constructed.^{2,6,17-25}

Bioelectrocatalysis, in which an enzyme reaction and an electrode reaction is coupled, is a key process for biofuel cells.¹⁻⁸ The reaction is classified into two types: mediated electron transfer

(MET) and direct electron transfer (DET). In the MET-type system, an artificial redox mediator shuttles electrons between an electrode and an enzyme. Regarding performance of biofuel cells, mediators can minimize the kinetic barrier in the electron transfer between redox enzymes and electrodes. However, this often incurs a thermodynamic loss in order to create a driving force for the electron transfer between an enzyme and an electrode, and thus often decreases the operating potential of biofuel cells.¹⁻⁸

Conversely, in DET-type systems, an enzyme directly communicates with an electrode. This makes it possible to construct a compact and simple biofuel cell and to minimize the thermodynamic loss in the electron transfer between an enzyme and an electrode.¹⁻⁸ Hydrogenase,^{11,15} fructose dehydrogenase (FDH),^{26,27} glucose dehydrogenase,²⁸ and cellobiose dehydrogenase^{29,30} are known to be enzymes capable of DET-type bioelectrocatalysis at bioanodes, and MCOs including bilirubin oxidase (BOD),³¹⁻³³ laccase,^{34,35} and Cu efflux oxidase^{36,37} are known to be DET-type enzymes for biocathodes. However, there are two major problems with DET-type biofuel cells: 1) Only a limited number of enzymes are suitable for DET-type bioelectrocatalysis; and 2) interfacial electron transfer kinetics between an enzyme and an electrode often becomes a kinetic bottleneck inducing large overpotentials.^{4,38-42} Since the interfacial electron transfer rate constant decreases exponentially with an increase in the tunneling distance between the active site of an enzyme and an electrode^{43,44}, the orientation of an adsorbed enzyme is one of the most important factors in controlling the interfacial electron transfer kinetics.^{4,38-42} Several approaches to realizing favorable enzyme

^a Division of Applied Life Sciences, Graduate School of Agriculture, Kyoto University, Sakyo, Kyoto 606-8502, Japan

E-mail: kano.kenji.5z@kyoto-u.ac.jp (K. Kano)

^b Department of Life Science, Graduate School of Life Science, University of Hyogo, 3-2-1 Koto, Kamigori-cho, Ako-gun, Hyogo 678-1297, Japan.

Electronic Supplementary Information (ESI) available: Electrochemical data and details of recent advancement in biofuel cells. See DOI: 10.1039/x0xx00000x

orientation have been proposed, such as genomic enzyme modification,^{45,46} electrode modification,^{42,47-58} and screening of suitable electrode materials.⁵⁹⁻⁶²

Generally, MCOs have four Cu atoms as active sites (labeled as types I, II, and III based on their spectroscopic and magnetic properties).¹⁰ Type I Cu and type II-III Cu clusters are known as the electron-accepting site and the catalytic site for $4e^-$ reduction of O_2 , respectively.^{10,63,64} Among the MCOs, BOD is a promising enzyme for DET-type biocathodes.³¹⁻³³ BOD has high bioelectrocatalytic activity even at neutral pH, and its formal potential ($E^{o'}_{E} = 0.46V$ vs. $Ag|AgCl|sat. KCl$ at pH 7) is relatively close to that of the $2H_2O/O_2$ redox couple ($E^{o'}_{O} = 0.62 V$ vs. $Ag|AgCl|sat. KCl$ at pH 7).⁶⁵ The modification of electrodes and utilization of compatible electrode materials have been reported as effective methods to improve the interfacial electron transfer of BODs.^{42,54-58,60,61} These methods include covalent modification by diazonium coupling⁵⁴ or oxidation of amines,⁴² physical adsorption of bilirubin⁵⁵⁻⁵⁷ or other aromatic compounds,⁵⁸ and utilization of functionalized carbon nanotubes (CNTs) such as pyrene-functionalized CNTs⁶⁰ and water-soluble CNTs with lengths of 1–4 μm .⁶¹

O_2 -tolerant and O_2 -sensitive [NiFe]-hydrogenases are often utilized for DET-type bioanodes.^{2,6,17-25} In H_2 oxidation, H_2 binding to the Ni-SI state (active silent state) is the first step, and subsequently the catalytic cycle proceeds to the Ni-R (H_2 -reduced state), Ni-C (one-electron-oxidized state of Ni-R), and Ni-SI states in turn.^{11,15,16} In the presence of O_2 , however, [NiFe]-hydrogenases become inactive.^{11,15,16} Ni-A state (also termed the “unready” or irreversible inactive state) and Ni-B state (also termed the “ready” or reversible inactive state) have been reported.^{11,15,16} The Ni-A state seems to be produced by one-electron oxidation of the Ni-SI state, in which a peroxide ligand is thought to coordinate to the Ni atom in the bridging position with respect to Fe(II).^{11,15,16} However, there has been much debate concerning the oxygenation of sulfur atoms near the active site in recent literature.⁶⁶ The Ni-B state is also produced by one-electron oxidation of the Ni-SI state, in which, in contrast to the Ni-A state, a hydroxide ligand is coordinated to the Ni atom in the bridging position with respect to Fe(II).^{11,15,16} The O_2 -tolerant mechanism has been considered due to the presence of a unique [FeS]-cluster close to the active site (i.e., a [4Fe-3S]-cluster coordinated by six Cys residues rather than a [4Fe-4S]-cluster coordinated by four Cys residues, as in other [NiFe]-hydrogenases) that transfers two electrons rapidly to the active site when the hydrogenase is attacked by O_2 .⁶⁷⁻⁷⁰ This property seems to enable O_2 -tolerant [NiFe]-hydrogenases to form the Ni-B inactive state only under oxidative conditions.^{11,39,71} Conversely, O_2 -sensitive [NiFe]-hydrogenases form both of the inactive states (Ni-A and Ni-B states) under oxidative conditions.^{11,15,16}

With regard to DET-type bioelectrocatalysis of hydrogenases, O_2 -tolerant [NiFe]-hydrogenase⁷²⁻⁷⁵ is specialized to H_2 oxidation and needs an overpotential for bioelectrochemical H_2 -oxidation. Conversely, O_2 -sensitive [NiFe]-hydrogenase^{76,77} can realize a reversible and bidirectional catalytic reaction (H_2 oxidation and H^+ reduction), and the zero-current potential of the electrode is almost identical to the equilibrium potential of the $H_2/2H^+$ couple.³⁹

Generally, electrode potentials that are high compared with the formal potential of the enzymes are required for bioanodes to achieve high-speed and enzyme-kinetics-controlled DET-type

bioelectrocatalysis.⁷⁸ However, [NiFe]-hydrogenases suffer from high oxidative stress at such high potentials and inactive states (Ni-A and Ni-B states) are produced. This phenomena is called oxidative inactivation,^{41,79-81} and causes power decay in H_2/O_2 biofuel cells. Schuhmann et al. and Lubitz et al. have proposed a new strategy to protect hydrogenases against oxidative inactivation in MET-type systems using a specifically designed viologen-based redox hydrogel.⁸² Electron transfer between the polymer-bound viologen moieties controls the potential near the active site of the hydrogenase, and thus the redox hydrogel insulates the enzyme from excessive oxidative stress.⁸²

Combining a MCO-adsorbed biocathode and [NiFe]-hydrogenase-adsorbed bioanode, we can construct a DET-type H_2/O_2 biofuel cell.^{2,6,17-25} The low solubility of the gaseous substrates (H_2 and O_2) frequently causes a power decline. To solve this problem, a gas diffusion electrode that can supply a gaseous substrate to an enzyme from the gas phase has been proposed.^{25,56,80,83-87} In addition, the gas diffusion electrode can maintain high substrate concentrations near the active enzyme on the electrode. This system is also useful for avoiding the aforementioned oxidative inactivation of [NiFe]-hydrogenases, since the inactivation is thought to compete with H_2 binding to the Ni-SI state.^{80,85} Furthermore, the gas diffusion electrode allows independent supply of gaseous substrates to the bioanode and the biocathode, thus avoiding the risk of explosion on mixing of H_2 with and O_2 , as reported in the literature.¹⁹

In this study, we investigated waterproof carbon material as an electrode base in order to realize high gas permeability and created a new type of gas diffusion electrode. BOD and two kinds of [NiFe]-hydrogenases (O_2 -tolerant and O_2 -resistant) were used to modify the electrode, and the resulting electrochemical properties were assessed. Finally, we constructed a DET-type dual gas diffusion H_2/O_2 biofuel cell system, which is the first example of such in the field of biofuel cells.

Experimental

Chemicals

Waterproof carbon cloth (WPCC, EC-CC1-060T) was purchased from Toyo Corp., (Japan), and Ketjen black EC300J (KB) was kindly donated by Lion Corp., (Japan). Poly(1,1,2,2-tetrafluoroethylene) (PTFE, 6-J) fine powder was purchased from DuPont-Mitsui Fluorochemicals Co., Ltd., (Japan). Bilirubin was purchased from Wako Pure Chemical (Japan) and was dissolved in 30 mM NaOH aqueous solution. BOD (EC 1.3.3.5) from *Myrothecium verrucaria* was donated by Amano Enzyme Inc. (Japan) and used without further purification. O_2 -tolerant membrane-bound [NiFe]-hydrogenase from *Hydrogenovibrio marinus* (HmMBH) and O_2 -sensitive [NiFe]-hydrogenase from *Desulfovibrio vulgaris* Miyazaki F (DvMF) were purified according to the literature.^{75,88} All other chemicals used in this study were of analytical grade unless otherwise specified, and all aqueous solutions were prepared with distilled water.

Electrode preparation

The gas diffusion electrode was prepared as follows: KB powder (40 mg) was mixed with PTFE and homogenized in 3.5 mL of 2-propanol

for 3 min at 0 °C to prepare a KB slurry. Then, about 1.0 mL of the KB slurry was applied to one side of a 1.4 cm² piece of WPCC and dried. This electrode is termed KB/PTFE/WPCC. Bilirubin modification of KB/PTFE/WPCC was carried out according to the literature with minor modifications.⁵⁶ Briefly, 0.3 mL of bilirubin solution (1 mM) was applied to a KB/PTFE/WPCC electrode, which was previously dried at 60 °C, and the surface was washed with 10 mM phosphate buffer (pH 7) five times. The bilirubin-modified electrode is termed BL/KB/PTFE/WPCC.

A 0.3 mL aliquot of BOD solution (20 mg mL⁻¹) dissolved in 10 mM phosphate buffer (pH 7) was applied to the surface of a KB/PTFE/WPCC electrode and a BL/KB/PTFE/WPCC electrode. A 0.3 mL aliquot of *Hm*MBH solution (5 mg mL⁻¹) dissolved in 10 mM phosphate buffer (pH 7, containing 0.2 M NaCl and 0.025% Triton X-100) was applied to a KB/PTFE/WPCC electrode, and 0.3 mL of *Dv*MF solution (5 mg mL⁻¹) dissolved in 25 mM Tris-HCl buffer (pH 7.4) was applied to a further KB/PTFE/WPCC electrode. These electrodes were dried for 2 h under reduced pressure at room temperature.

Electrochemical measurements

Cyclic voltammetry and chronoamperometry were carried out on BAS CV50W and ALS 714C electrochemical analyzers, respectively. A handmade gas-diffusion-type electrolysis cell identical to that reported in a previous paper was used for the measurements.⁵⁶ The projected surface area of the working electrode was set to 1.0 cm². A Ti mesh served as a current collector. A Pt mesh and an Ag|AgCl|sat. KCl electrode were used as counter and reference electrodes, respectively. All potentials in this study are in reference to the reference electrode. The measurements were performed in 1.5 M citrate buffer (pH 5) at 40 °C under quiescent conditions, with O₂ and H₂ atmospheres at the biocathodes and bioanodes, respectively.

DET-type biofuel cells

Chronopotentiometry was carried out on an HA-151A (Hokuto

Denko) electrochemical analyzer to evaluate the performance of the bioanode (*Dv*MF-adsorbed KB/PTFE/WPCC) and the biocathode (BOD-adsorbed BL/KB/PTFE/WPCC). The aforementioned gas-diffusion-type electrolysis cell identical to that reported in a previous paper⁵⁶ was used for the measurements. For practical application, it is normal to evaluate a cell performance using a one-compartment cell. However, complete separation of the H₂ and O₂ outlet gases was difficult in our experimental system. Thus, for safety, we evaluated each of the single electrodes of the DET-type H₂/O₂ biofuel cell separately, but under the same conditions (except the flow gas, which was H₂ for the bioanode and O₂ for the biocathode).

Results and discussion

Optimization of KB/PTFE/WPCC with BOD

Figure 1 shows cyclic voltammograms (CVs) for the BOD-adsorbed KB/PTFE/WPCC (black line) and the BOD-adsorbed BL/KB/PTFE/WPCC (gray line) under quiescent and O₂ (solid lines) or Ar (dotted line) atmospheric conditions. The PTFE content was 50% (PTFE/PTFE+KB (wt%)) and the bilirubin concentration was 3 mM. The faradic waves are ascribed to O₂ reduction due to DET-type bioelectrocatalysis with BOD, as described in the literature.^{32,42,54-58,60,61}

The BOD-adsorbed BL/KB/PTFE/WPCC exhibits a clear catalytic wave with sigmoidal shape compared with the BOD-adsorbed KB/PTFE/WPCC. Modification with bilirubin is an effective way to induce a favorable orientation of the BOD,⁵⁵⁻⁵⁷ and this characteristic indicates that the interfacial electron transfer between BOD and BL/KB/PTFE/WPCC is faster than that between BOD and KB/PTFE/WPCC. In the case of KB/PTFE/WPCC, the most favorable BOD adsorption is realized by setting the bilirubin concentration to 3 mM (Fig. S1).

The inset of Fig. 1 shows a chronoamperogram (CA) at 0 V for the BOD-adsorbed KB/PTFE/WPCC. A steady-state catalytic reduction current at a current density of -25 mA cm⁻² is obtained until about 15 s. However, the catalytic reduction current gradually

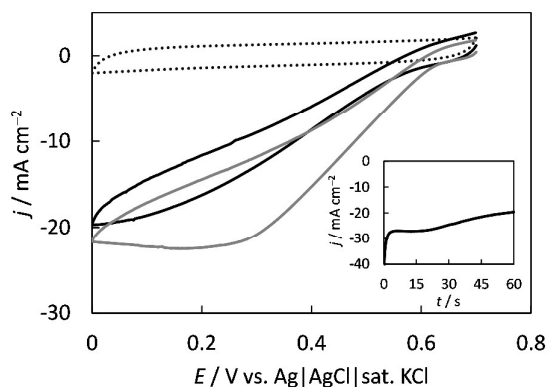


Fig. 1 CVs for BOD-adsorbed KB/PTFE/WPCC (black line) and BL/KB/PTFE/WPCC (gray line). The scan rate was 10 mV s⁻¹. The inset shows CA for BOD-adsorbed KB/PTFE/WPCC. The electrode potential was 0 V. Measurements were carried out in 1.5 M citrate buffer (pH 5) at 40 °C under quiescent and O₂ (solid lines) or Ar (dotted line) atmospheric conditions. The PTFE content and the bilirubin concentration were 50% and 3 mM, respectively.

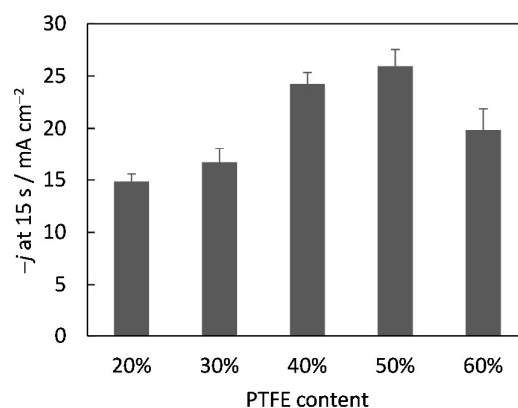


Fig. 2 Effects of the PTFE content on the steady-state catalytic reduction current densities after 15 s in CA at 0 V. Measurements were carried out in 1.5 M citrate buffer (pH 5) at 40 °C under quiescent and O₂ atmospheric conditions. The error bars were evaluated by the Student *t* distribution at a 90% confidence level.

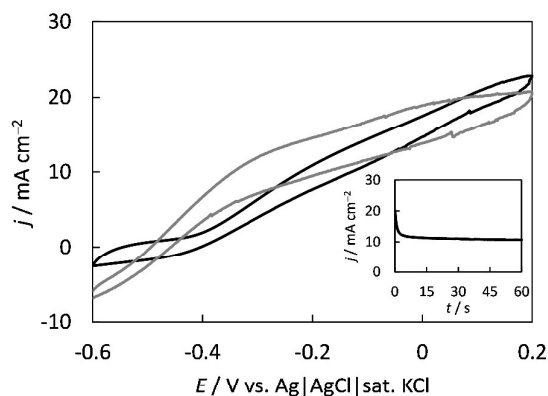


Fig. 3 CVs of *HmMBH*- and *DvMF*-adsorbed KB/PTFE/WPCC (black and gray lines, respectively). The scan rate was 10 mV s^{-1} . The inset shows the CA of *HmMBH*-adsorbed KB/PTFE/WPCC. The electrode potential was -0.1 V . Measurements were carried out in 1.5 M citrate buffer (pH 5) at $40 \text{ }^\circ\text{C}$ under quiescent and H_2 atmospheric conditions. The PTFE content was 50%.

decreases with time. Similar phenomena are observed even when the O_2 gas is blown forcibly onto the surface of the electrode (Fig. S2). These results indicate that the current decrease is not caused by O_2 depletion near the electrode surface. In addition, as shown in Fig. S3, repeated CAs (by setting the electrode to open-circuit for 5 min before the second and third measurements) exhibit similar results. It should be noted here that the steady-state reduction current is return to the initial value in the first chronoamperometric experiment. This indicates that the enzyme remains active for long time. The decrease in the current is most likely due to a slight change in balance of bio-three-phase balance that will be regulated by the electrode hydrophilicity/hydrophobicity and the H_2O amount (including a balance of generation and vaporization of H_2O). Since the reduction currents after 15 s in the CAs are controlled by the gas permeability, we selected them as an index to optimize the PTFE content. The catalytic reduction current densities at the BOD-adsorbed KB/PTFE/WPCC with various PTFE contents are summarized in Fig. 2. The optimum PTFE content for the BOD-adsorbed KB/PTFE/WPCC is 50%, and the reduction current densities reach 26 ± 2 and $17 \pm 3 \text{ mA cm}^{-2}$ after 15 and 60 s, respectively (note here that the errors in this study were evaluated by the Student t distribution at a 90% confidence level). The performance is much better than that previously reported for DET-type O_2 reduction with gas-diffusion-type electrodes (about 13 mA cm^{-2}).⁸⁷ Accordingly, we succeeded in constructing a DET-type gas diffusion bioelectrode with high gas permeability.

Gas-diffusion-type H_2 oxidation with [NiFe]-hydrogenases

We utilized *HmMBH* and *DvMF* as catalysts for H_2 oxidation. As shown in Fig. S4, characteristic rotating disk voltammograms are observed for *HmMBH*- and a *DvMF*-adsorbed KB-modified electrodes. The rotating disk mode was used to avoid concentration depletion near the electrode surface. In the case of the *HmMBH*-adsorbed electrode (black line), an H_2 -oxidation wave is observed and the current gradually decreases at positive potentials due to

oxidative stress (i.e., oxidative inactivation, as discussed in the Introduction section). The apparent half-wave potential of the sigmoidal part of the steady-state wave ($E_{1/2}' = -0.39 \text{ V}$) is slightly more positive than the formal potential of the $\text{H}_2/2\text{H}^+$ redox couple at pH 6 ($E_{\text{H}^+}^{\text{or}} = -0.53 \text{ V}$). The overpotential ($= E_{1/2}' - E_{\text{H}^+}^{\text{or}}$) is predominantly ascribed to the difference between $E_{\text{H}^+}^{\text{or}}$ and the formal potential (E_{E}^{or}) of the catalytic center of *HmMBH*.⁴¹ The *DvMF*-adsorbed electrode (gray line) exhibits a reversible and bidirectional catalytic wave, i.e., H_2 oxidation at positive potentials and H^+ reduction at negative potentials.⁷⁷ $E_{1/2}'$ is -0.51 V and close to $E_{\text{H}^+}^{\text{or}} = -0.53 \text{ V}$. This means that the bioelectrocatalytic conversion between $\text{H}_2/2\text{H}^+$ does not require any overpotential. However, the oxidation current rapidly decreases at positive potentials due to oxidative inactivation.

Conversely, we report that the oxidative inactivation can be suppressed by using a gas diffusion system.^{80,85} Figure 3 shows CVs of the *HmMBH*- (black line) and the *DvMF*-adsorbed KB/PTFE/WPCC (gray line) under quiescent and H_2 atmospheric conditions. The PTFE content was set as 50%, as optimized in the above section (Fig. 2). The oxidation current densities at the *HmMBH*-adsorbed KB/PTFE/WPCC continue to increase with the potential and reach a value of about 20 mA cm^{-2} at 0.2 V . The *HmMBH*-adsorbed KB/PTFE/WPCC retains a large steady-state oxidation current density of 10 mA cm^{-2} at -0.1 V according to CA (Fig. 3, inset). We can conclude that the H_2 supply is sufficient to suppress the oxidative inactivation of *HmMBH* adsorbed on the KB/PTFE/WPCC at -0.1 V and to produce a large current density.

At the *DvMF*-adsorbed KB/PTFE/WPCC, slight inactivation is still observed at potentials over 0.1 V (Fig. 3, gray line). However, multi-sweep CVs between -0.6 and -0.3 V show almost constant bioelectrocatalysis with a limiting current density of about 10 mA cm^{-2} (Fig. S5). This result suggests that the oxidative inactivation is largely prevented at the *DvMF*-adsorbed KB/PTFE/WPCC in this potential range (up to -0.3 V). *DvMF* (classified as O_2 -sensitive) catalyzes the reversible and bidirectional H_2 oxidation and H^+ reduction and is able to catalyze electrochemical H_2 oxidation without overpotential (Fig. S4). Consequently, we utilized *DvMF* (as well as BOD) to construct a DET-type H_2/O_2 biofuel cell.

DET-type dual gas diffusion H_2/O_2 biofuel cells

We constructed a dual gas diffusion H_2/O_2 biofuel cell with *DvMF*-adsorbed KB/PTFE/WPCC and BOD-adsorbed BL/KB/PTFE/WPCC as the bioanode and biocathode, respectively. Normally, both the bioanode and the biocathode are placed in the biofuel cell assembly, and the polarization curve is obtained by changing the resistance between the anode and the cathode.^{2,6} However, due to possible gas leakage from the biofuel cells and the commensurate risk of explosion, it is dangerous to operate a dual gas diffusion H_2/O_2 biofuel cell in a conventional experimental situation. Thus, in this study, the performances of the bioanode and the biocathode were evaluated separately by chronopotentiometry (CP) for 15 s under the same conditions except for the flow gas (H_2 and O_2 gas were supplied to the bioanode and the biocathode, respectively). In our experience with H_2/O_2 biofuel cells, the polarization curve of a biofuel cell assembly is almost identical to that obtained when the bioanode and the biocathode are evaluated separately.¹⁷

Potentiograms of the *Dv*MF-adsorbed KB/PTFE/WPCC and the BOD-adsorbed BL/KB/PTFE/WPCC are shown in Fig. S6 (A) and (B). Although the potentials change gradually under large current densities (e.g., 15 mA cm⁻² for the anode and 28 mA cm⁻² for the cathode), the potentials at lower current densities show steady-state characteristics. Figure 4 (A) shows the potentials of the bioanode and the biocathode in CP recorded 15 s after closing the circuit as a function of the current density. Figure 4 (B) shows the current density dependences of the cell voltage and the cell power density calculated from the data in Fig. 4 (A). The open-circuit voltage is 1.14 ± 0.03 V and is close to the standard motive force of the ideal H₂/O₂ cell (1.23 V). The maximum power density is 8.4 ± 0.5 mW cm⁻² at 0.7 V of the cell voltage. The power density can be compared with that of a recent polymer electrolyte H₂/O₂ fuel cell with Pt as the catalyst (68 mW cm⁻² at 0.21 V at 1 atm, 40 °C, in a membrane-electrode assembly system with single cell).¹⁴

Since the effects of oxidative inactivation on the current increase for high current densities at the bioanode, it is difficult to correctly evaluate the cell performance for current densities above 15 mA cm⁻². However, we can certainly report that a powerful H₂/O₂ DET-type biofuel cell with dual gas diffusion has been successfully constructed.

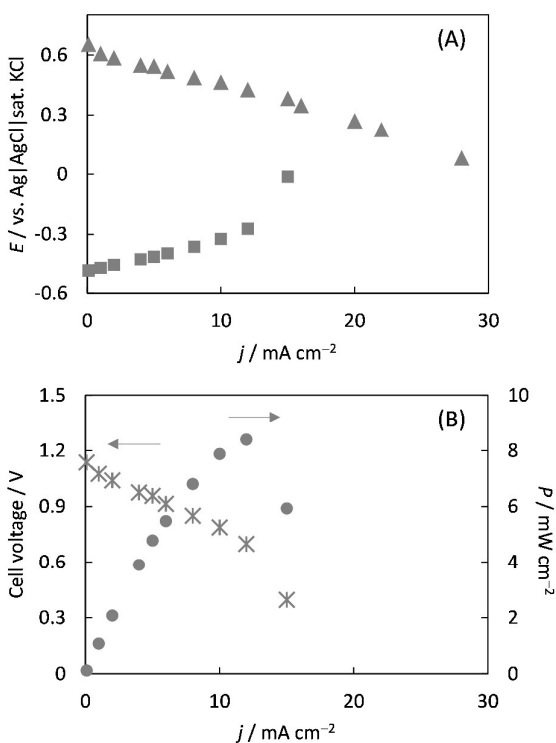


Fig. 4 (A) Polarization curves of a DET-type dual gas diffusion H₂/O₂ biofuel cell. The potentials of the bioanode and the biocathode as measured in CP are plotted as functions of the current density. The measurements were carried out in 1.5 M citrate buffer (pH 5) at 40 °C under quiescent and H₂ and O₂ atmospheric conditions for the bioanode or the biocathode, respectively. (B) The cell voltage and the power density as a function of the current density of the biofuel cell.

Figure 5 summarizes recent developments in the power densities of H₂/O₂ biofuel cells (in both MET- and DET-type systems) and DET-type biofuel cells with other fuels as reported in the literature.^{2,6,89-91} The details are summarized in Table S1. The data for biofuel cells utilizing Pt as the cathode catalyst are not included, because we attempted to comprehensively compare the performance of the biofuel cells with the bioanode and the biocathode. As judged from Fig. 5 (and Table S1), the performance of our biofuel cell is 5.6 times better than that of the best H₂/O₂ biofuel cell in the literature and 3.2 times larger than that of DET-type biofuel cells with other fuels.

Since the concentrations of H₂ and O₂ in solution are proportional to the partial pressures of the H₂ and O₂ gases, it is impossible to realize a saturated condition for both gases without a separator in the solution.^{17,20,22,24} In addition, the risk of explosion on mixing the H₂ and O₂ gases is debated.¹⁹ Gas diffusion electrodes avoid these problems.²⁵ By constructing gas diffusion electrodes for the bioanode and the biocathode, we are able to completely separate the H₂ and O₂ gas inlets and realize high concentrations of the gas substrates for both the bioanode and the biocathode.

From the viewpoint of DET-type biofuel cells with other fuels, FDH is a promising catalyst for bioanodes,^{56,59,83,89,90} since FDH has a high DET-type bioelectrocatalytic activity and exhibits about 40 mA cm⁻² at porous carbon electrodes.⁵⁶ However, its maximum power density is limited to 2.6 mW cm⁻² (6 mA cm⁻² at 0.45 V of the cell voltage) due to a large overpotential ascribed to thermodynamic loss in the electron transfer from the substrate (D-fructose) to FDH and a kinetic barrier in the electron transfer from FDH to the electrode.^{27,38} Conversely, $E_{1/2}'$ of the catalytic wave on the *Dv*MF-adsorbed KB/PTFE/WPCC is close to $E_{H^+}^0$ thanks to the reversible characteristics of *Dv*MF and fast interfacial electron transfer kinetics. Consequently, these characteristics contribute to the realization of high operating potential, which results in a high power density.

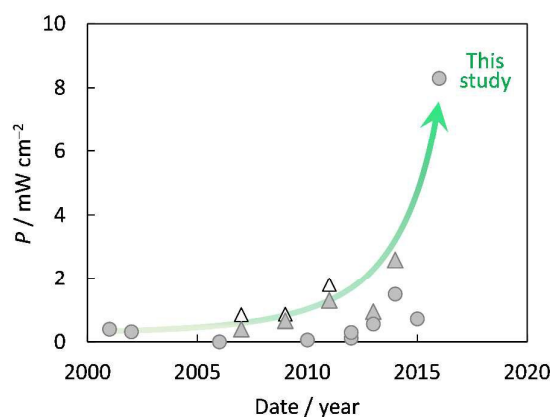


Fig. 5 Recent advancement in the power density of H₂/O₂ biofuel cells and DET-type biofuel cells. The power densities of H₂/O₂ biofuel cells and DET-type biofuel cells with other fuels are indicated with circles and triangles, respectively. The open triangles are the values evaluated under stirring conditions. Power densities measured from a single-layer cell with identical bioanode and the biocathode surface areas are presented to fairly compare their performances. The details are summarized in Table S1.

Conclusions

A novel gas diffusion bioelectrode fabricated with WPCC was created and optimized. The electrode showed a high gas permeability, which realized steady-state catalytic current densities as large as 10 mA cm⁻² for H₂ oxidation and O₂ reduction. For the biocathode, the electron transfer between BOD and the KB/PTFE/WPCC was accelerated by bilirubin modification.⁵⁶ For the bioanode, the gas diffusion electrode greatly suppressed the oxidative inactivation of HmMBH and DvMF. By combining the DvMF-adsorbed KB/PTFE/WPCC and the BOD-adsorbed BL/KB/PTFE/WPCC, we succeeded in constructing a DET-type dual gas diffusion H₂/O₂ biofuel cell. This is the first report of a dual gas-diffusion system in the field of biofuel cells, and enables us to separately supply the gas substrates (H₂ or O₂) from the gas phases of the bioanode and the biocathode. Therefore, it becomes possible to independently control the substrate supply to the bioanode and the biocathode. The cell exhibited a power density of 8.4 mW cm⁻² at 0.7 V of the cell voltage under quiescent conditions by flowing the H₂ and O₂ gases into the gas phases of the bioanode and biocathode, respectively. This value is 5.6 and 3.2 times larger than those of the best reported H₂/O₂ biofuel cell and the best DET-type biofuel cell with other fuels, respectively.

Acknowledgements

This work was supported by Core Research for Evolutional Science and Technology, Japan Science and Technology Agency (to Y. H. and K. K.) and Research Fellowships of Japan Society for the Promotion of Science for Young Scientists #15J02900 (to K. S.). The authors would like to thank Lion Corp. and Amano Enzyme Inc. for their kind donations of KB and BOD, respectively, and also Enago (www.enago.jp) for the English language review.

References

- S. C. Barton, J. Gallaway and P. Atanassov, *Chem. Rev.*, 2004, **104**, 4867.
- A. D. Poulpique, D. Ranava, K. Monsalve, M. Giudici-Ortoni and E. Lojou, *ChemElectroChem*, 2014, **1**, 1724.
- D. Leech, P. Kavanagh and W. Schuhmann, *Electrochim. Acta*, 2012, **84**, 223.
- C. Léger and P. Bertrand, *Chem. Rev.*, 2008, **108**, 2379.
- N. Mano, F. Mao and A. Heller, *ChemBioChem*, 2004, **5**, 1703.
- M. Rasmussen, S. Abdellaoui and S. D. Minteer, *Biosens. Bioelectron.*, 2016, **76**, 91.
- J. A. Cracknell, K. A. Vincent and F. A. Armstrong, *Chem. Rev.*, 2008, **108**, 2439.
- M. Zhou, *Electroanalysis*, 2015, **27**, 1786.
- A. Kietzin and M. W. W. Adams, *FEMS Microbiol. Rev.*, 1996, **18**, 5.
- E. I. Solomon, U. M. Sundaram and T. E. Machonkin, *Chem. Rev.*, 1996, **96**, 2563.
- K. A. Vincent, A. Parkin and F. A. Armstrong, *Chem. Rev.*, 2007, **107**, 4366.
- B. C. H. Steele and A. Heinzl, *Nature*, 2001, **414**, 345.
- M. Z. Jacobson, W. G. Colella and D. M. Golden, *Science*, 2005, **308**, 1901.
- M. R. Berber, T. Fujigaya, K. Sasaki and N. Nakashima, *Sci. Rep.*, 2013, **3**, 1764.
- H. S. Shafaat, O. Rüdiger, H. Ogata and W. Lubitz, *Biochim. Biophys. Acta*, 2013, **1827**, 986.
- T. Yagi and Y. Higuchi, *Proc. Jpn. Acad. Ser. B*, 2013, **89**, 16.
- S. Tsujimura, M. Fujita, H. Tatsumi, K. Kano and T. Ikeda, *Phys. Chem. Chem. Phys.*, 2001, **3**, 1331.
- M. R. Tarasevich, V. A. Bogdanovskaya, N. M. Zagudaeva and A. V. Kapustin, *Russ. J. Electrochem.*, 2002, **38**, 335.
- K. A. Vincent, J. A. Cracknell, J. R. Clark, M. Ludwig, O. Lenz, B. Friedrich and F. A. Armstrong, *Chem. Commun.*, 2006, 5033.
- A. F. Wait, A. Parkin, G. M. Morley, L. D. Santos and F. A. Armstrong, *J. Phys. Chem. C*, 2010, **114**, 12003.
- S. Krishnan and F. A. Armstrong, *Chem. Sci.*, 2012, **3**, 1015.
- A. Ciaccava, A. D. Poulpique, V. Techer, M. T. Giudici-Ortoni, S. Tingry, C. Innocent and E. Lojou, *Electrochem. Commun.*, 2012, **23**, 25.
- L. Xu and F. A. Armstrong, *Energy Environ. Sci.*, 2013, **6**, 2166.
- A. D. Poulpique, A. Ciaccava, R. Gadiou, S. Gounel, M. T. Giudici-Ortoni, N. Mano and E. Lojou, *Electrochem. Commun.*, 2014, **42**, 72.
- N. Lalaoui, A. D. Poulpique, R. Haddad, A. L. Goff, M. Holzinger, S. Gounel, M. Mermoux, P. Infossi, N. Mano, E. Lojou and S. Cosnier, *Chem. Commun.*, 2015, **51**, 7447.
- S. Kawai, M. Goda-Tsutsumi, T. Yakushi, K. Kano and K. Matsushita, *Appl. Environ. Microbiol.*, 2013, **79**, 1654.
- S. Kawai, T. Yakushi, K. Matsushita, Y. Kitazumi, O. Shirai and K. Kano, *Electrochem. Commun.*, 2014, **38**, 28.
- V. Flexer, F. Durand, S. Tsujimura and N. Mano, *Anal. Chem.*, 2011, **83**, 5721.
- A. Lindgren, L. Gorton, T. Ruzgas, U. Baminger, D. Haltrich and M. Schüle, *J. Electroanal. Chem.*, 2001, **496**, 76.
- V. Fridman and U. Wollenberger, V. Bogdanovskaya, F. Lisdat, A. Lindfren, L. Gorton and F. W. Scheller, *Biochem. Soc. Trans.*, 2000, **28**, 63.
- S. Murao and N. Tanaka, *Agric. Biol. Chem.*, 1981, **45**, 2383.
- S. Tsujimura, T. Nakagawa, K. Kano and T. Ikeda, *Electrochemistry*, 2004, **72**, 437.
- N. Mano and L. Edembe, *Biosens. Bioelectron.*, 2013, **50**, 478.
- M. R. Tarasevich, A. I. Yaropolov, V. A. Bogdanovskaya and S. D. Varfolomeev, *J. Electroanal. Chem.*, 1979, **104**, 393.
- S. Shleev, A. Jarosz-Wilkolazka, A. Khalunina, O. Morozova, A. Yaropolov, T. Ruzgas and L. Gorton, *Bioelectrochemistry*, 2005, **67**, 115.
- K. Kataoka, H. Komori, Y. Ueki, Y. Konno, Y. Kamitaka, S. Kurose, S. Tsujimura, Y. Higuchi, K. Kano, D. Seo and T. Sakurai, *J. Mol. Biol.*, 2007, **373**, 141.
- Y. Miura, S. Tsujimura, S. Kurose, Y. Kamitaka, K. Kataoka, T. Sakurai and K. Kano, *Fuel Cells*, 2009, **9**, 70.
- C. Léger and A. Jones, S. P. J. Albracht and F. A. Armstrong, *J. Phys. Chem. B*, 2002, **106**, 13058.
- C. Léger, A. K. Jones, W. Roseboom, S. P. J. Albracht and F. A. Armstrong, *Biochemistry*, 2002, **41**, 15736.
- V. Fourmond, C. Baffert, K. Sybirna, T. Lautier, A. A. Hamdan, S. Dementin, P. Soucaille, I. Meynial-Salles, H. Bottin and C. Léger, *J. Am. Chem. Soc.*, 2013, **135**, 3926.
- K. So, R. Hamamoto, R. Takeuchi, Y. Kitazumi, O. Shirai, R. Endo, H. Nishihara, Y. Higuchi and K. Kano, *J. Electroanal. Chem.*, 2016, **766**, 152.
- H. Xia, Y. Kitazumi, O. Shirai and K. Kano, *J. Electroanal. Chem.*, 2016, **763**, 104.
- C. C. Page, C. C. Moser, X. Chen and P. L. Dutton, *Nature*, 1999, **402**, 47.
- R. A. Marcus, *Angew. Chem. Int. Ed.*, 1993, **32**, 1111.

- 45 V. Balland, C. Hureau, A. M. Cusano, Y. Liu, T. Tron and B. Limoges, *Chem. Eur. J.*, 2008, **14**, 7186.
- 46 M. Sosna, H. Boer and P. N. Bartlett, *ChemPhysChem*, 2013, **14**, 2225.
- 47 P. Olejnik, B. Palys, A. Kowalczyk and A. M. Nowicka, *J. Phys. Chem. C*, 2012, **116**, 25911.
- 48 M. T. Meredith, M. Minson, D. Hickey, K. Artyushkova, D. T. Glatzhofer and S. D. Minteer, *ACS Catal.*, 2011, **1**, 1683.
- 49 K. Stolarczyk, M. Sepelowska, D. Lyp, K. Zelechowska, J. F. Biernat, J. Rogalski, K. D. Farmer, K. N. Roberts and R. Bilewicz, *Bioelectrochemistry*, 2012, **87**, 154.
- 50 C. F. Blanford, R. S. Heath and F. A. Armstrong, *Chem. Commun.*, 2007, 1710.
- 51 M. Pita, C. Gutierrez-Sanchez, D. Olea, M. Velez, C. Garcia-Diego, S. Shleev, V. M. Fernandez and A. L. De Lacey, *J. Phys. Chem. C*, 2011, **115**, 13420.
- 52 C. Vaz-Dominguez, S. Campuzano, O. Rüdiger, M. Pita, M. Gorbacheva, S. Shleev, V. M. Fernandez and A. L. De Lacey, *Biosens. Bioelectron.*, 2008, **24**, 531.
- 53 V. Balland, C. Hureau, A. M. Cusano, Y. Liu, T. Tron and B. Limoges, *Chem. Eur. J.*, 2008, **14**, 7186.
- 54 L. D. Santos, V. Climent, C. F. Blanford and F. A. Armstrong, *Phys. Chem. Chem. Phys.*, 2010, **12**, 13962.
- 55 J. A. Cracknell, T. P. McNamara, E. D. Lowe and C. F. Blanford, *Dalton Trans.*, 2011, **40**, 6668.
- 56 K. So, S. Kawai, Y. Hamano, Y. Kitazumi, O. Shirai, M. Hibi, J. Ogawa and K. Kano, *Phys. Chem. Chem. Phys.*, 2014, **16**, 4823.
- 57 R. J. Lopez, S. Babanova, Y. Ulyanova, S. Singhal and P. Atanassov, *ChemElectroChem*, 2014, **1**, 241.
- 58 G. Göbel and F. Lisdat, *Electrochem. commun.*, 2008, **10**, 1691.
- 59 T. Miyake, S. Yoshino, T. Yamada, K. Hata and M. Nishizawa, *J. Am. Chem. Soc.*, 2011, **133**, 5129.
- 60 M. Jönsson-Niedziolka, A. Kaminska and M. Opallo, *Electrochim. Acta*, 2010, **55**, 8744.
- 61 K. So, M. Onizuka, T. Komukai, Y. Kitazumi, O. Shirai and K. Kano, *Electrochim. Acta*, 2016, **192**, 133.
- 62 C. Gutiérrez-Sánchez, M. Pita, C. Vaz-Domínguez, S. Shleev and A. L. D. Lacey, *J. Am. Chem. Soc.*, 2012, **134**, 17212.
- 63 S. Shleev, J. Tkac, A. Christenson, T. Ruzgas, A. I. Yaropolov, J. W. Whittaker and L. Gorton, *Biosens. Bioelectron.*, 2005, **20**, 2517.
- 64 K. Kataoka, R. Sugiyama, S. Hirota, M. Inoue, K. Urata, Y. Minagawa, D. Seo and T. Sakurai, *J. Biol. Chem.*, 2009, **284**, 14405.
- 65 S. Tsujimura, A. Kuriyama, N. Fujieda, K. Kano and T. Ikeda, *Anal. Biochem.*, 2005, **337**, 325.
- 66 A. Volbeda, L. Martin, P. Liebgott, A. L. D. Lacey and J. C. Fontecilla-Camps, *Metalomics*, 2015, **7**, 710.
- 67 T. Goris, A. F. Wait, M. Saggu, J. Fritsch, N. Heidary, M. Stein, I. Zebger, F. Lenz, F. A. Armstrong, B. Friedrich and O. Lenz, *Nat. Chem. Biol.*, 2011, **7**, 310.
- 68 M. Pandelia, W. Nitschke, P. Infossi, M. Giudici-Ortoni, E. Bill and W. Lubitz, *Proc. Natl. Acad. Sci. U. S. A.*, 2011, **108**, 6097.
- 69 M. M. Roessler, R. M. Evans, R. A. Davies, J. Harmer and F. A. Armstrong, *J. Am. Chem. Soc.*, 2012, **134**, 15581.
- 70 Y. Shomura, K. Yoon, H. Nishihara and Y. Higuchi, *Nature*, 2011, **479**, 253.
- 71 A. A. Hamdan, B. Burlat, O. Gutiérrez-Sanz, P. Liebgott, C. Baffert, A. L. D. Lacey, M. Rousset, B. Guigliarelli, C. Léger and S. Dementin, *Nat. Chem. Biol.*, 2013, **9**, 15.
- 72 J. Fritsch, P. Scheerer, S. Frielingsdorf, S. Kroschinsky, B. Friedrich, O. Lenz and C. M. T. Spahn, *Nature*, 2011, **479**, 249.
- 73 M. Pandelia, V. Fourmond, P. Tron-Infossi, E. Lojou, P. Bertrand, C. Léger, M. Giudici-Ortoni and W. Lubitz, *J. Am. Chem. Soc.*, 2010, **132**, 6991.
- 74 J. A. Cracknell, A. F. Wait, O. Lenz, B. Friedrich and F. A. Armstrong, *Proc. Natl. Acad. Sci. U. S. A.*, 2009, **106**, 20681.
- 75 K. Yoon, K. Fukuda, K. Fujisawa and H. Nishihara, *Int. J. Hydrogen Energy*, 2011, **36**, 7081.
- 76 A. K. Jones, E. Sillery, S. P. J. Albracht and F. A. Armstrong, *Chem. Commun.*, 2002, 866.
- 77 D. Millo, P. Hildebrandt, M. Pandelia, W. Lubitz and I. Zebger, *Angew. Chemie. Int. Ed.*, 2011, **50**, 2632.
- 78 A. J. Bard and L. R. Faulkner, *Electrochemical methods: fundamentals and applications*, 2nd ed., Wiley, New York.
- 79 A. A. Hamdan, P. Liebgott, V. Fourmond, O. Gutiérrez-Sanz, A. L. D. Lacey, P. Infossi, M. Rousset, S. Dementin and C. Léger, *Proc. Natl. Acad. Sci. U. S. A.*, 2012, **109**, 19916.
- 80 K. So, Y. Kitazumi, O. Shirai, K. Kurita, H. Nishihara, Y. Higuchi and K. Kano, *Bull. Chem. Soc. Jpn.*, 2014, **87**, 1177.
- 81 V. Fourmond, P. Infossi, M. Giudici-Ortoni, P. Bertrand and C. Léger, *J. Am. Chem. Soc.*, 2010, **132**, 4848.
- 82 N. Plumeré, O. Rüdiger, A. A. Oughli, R. Williams, J. Vivekananthan, S. Pöller, W. Schuhmann and W. Lubitz, *Nat. Chem.*, 2014, **6**, 822.
- 83 T. Miyake, K. Haneda, S. Yoshino and M. Nishizawa, *Biosens. Bioelectron.*, 2013, **40**, 45.
- 84 G. Gupta, C. Lau, V. Rajendran, F. Colon, B. Branch, D. Ivnitiski and P. Atanassov, *Electrochem. Commun.*, 2011, **13**, 247.
- 85 K. So, Y. Kitazumi, O. Shirai, K. Kurita, H. Nishihara, Y. Higuchi and K. Kano, *Chem. Lett.*, 2014, **43**, 1575.
- 86 S. C. Barton, *Electrochim. Acta*, 2005, **50**, 2145.
- 87 K. So, M. Onizuka, T. Komukai, Y. Kitazumi, O. Shirai and K. Kano, *Electrochem. Commun.*, 2016, **66**, 58.
- 88 Y. Higuchi, N. Yasuoka, M. Kakudo, Y. Katsube, T. Yagi, and H. Inokuchi, *J. Biol. Chem.*, 1987, **262**, 2823.
- 89 Y. Kamitaka, S. Tsujimura, N. Setoyama, T. Kajino and K. Kano, *Phys. Chem. Chem. Phys.*, 2007, **9**, 1793.
- 90 K. Murata, K. Kajiya, N. Nakamura and H. Ohno, *Energy Environ. Sci.*, 2009, **2**, 1280.
- 91 A. Zebda, C. Gondran, A. L. Goff, M. Holzinger, P. Cinquin and S. Cosnier, *Nat. Commun.*, 2011, **2**, 370.

